

Implementation of Non-Linear Control Strategy For Hybrid D-Statcom In Mitigation of Harmonics and Reactive Power Compensation

R Muralekrishnen¹, J Jayachandran² and S Malathi³

*¹PG-Scholar, ²Senior Assistant Professor, ³Assistant Professor
School of Electrical and Electronics Engineering, SASTRA University, Thanjavur-
613401, Tamilnadu, India
Email id: krishnaaa2020@gmail.com*

Abstract

This paper emphasis the combination of Thyristor-Controlled Reactor (TCR) and Shunt Hybrid Power Filter (SHPF) in PQ problems for mitigation of harmonics and reactive power consumption in the distribution system. The term Shunt Hybrid Power Filter denotes the combination of Passive filters and Active Power Filters. The combination of the TCR and the passive filter is technically termed as Shunt passive Filter which helps to improve the power factor by compensating the reactive power. The Active Power Filter is to mitigate the harmonics in the source current and to inhibit the hypothesis of resonance between the Shunt Passive Filter (SPF) and the line inductance. The TCR is controlled using proportional-integral controller and the corresponding triggering alpha value is educed from the lookup table to control the reactor value in the TCR. The Active Power Filter (APF) is controlled using non-linear control strategy. The simulation of the above model is carried out in MATLAB Simulink software for star and delta connected TCR and the %THD level of the source current is made to retain below 5%, which satisfies the IEEE-519Standard.

Index terms: Harmonic mitigation, Passive filter, Thyristor-Controlled Reactor (TCR), Active Power Filter (APF), Shunt Hybrid Power Filter (SHPF), Reactive power compensation, Non-Linear Controller.

Introduction

Most of the electrical devices in industries are using processed or regulated power to decrease the power consumptions and losses. In order to achieve this regulated power supply, the power electronics converters are mostly used. These power converters normally use rectifiers which are non-linear in nature and inject harmonics into

system current. The beingness of the harmonics at the system causes grievous problems such as overheating of transformers, harmonic resonance, switching losses and interference with the communication lines. Traditionally, the current harmonics in the supply network have been mitigated using Passive filters. Usage of these passive filters also has some restrains such as resonance effect. The reactive power in the system is compensated using different range of passive filters according to the requirement. The selection of passive filter is done with help of the power Thyristor. It is also termed as Thyristor Switched Filter (TSF). TSF is used to select the passive filter among the set of filters connected parallel according to the requirement of the reactive power. But this arrangement also suffers with parallel and series resonance which takes place amongst TSF and the grid. Active filters were designed to mitigate the difficulties raised with passive filters. The active filter is good at mitigating the current harmonics and gives better performance to the system. It costs more for the large scale systems because it requires higher rating power converter for its compensating process. Hence Hybrid filters which include passive filters as well as Active filters preferred. Hybrid filter includes the benefits of passive as well as active filters for mitigating the current harmonics and reactive compensation. The problems of the Active filter and Passive filter are softened efficaciously. And it offers cost-effective current harmonic mitigation for high power switching converters.

In this system, two types of loads are used. They are Linear Loads and Non-linear Loads. The Linear Load is simple three phase RLC load and Non-Linear Load is Power electronics switching circuit say Diode bridge rectifier. The system remains stable until linear loads are used. The system suffers with current harmonics as soon as Non-Linear load is introduced in it. This current harmonics makes the power quality very poor. The reactive power consumption also increases. This proposed system consists of Thyristor-Controlled Reactor (TCR) which is configured in Star connection and a shunted Hybrid Active Power Filter (SHPF) for the mitigation of harmonics in the system current and for the reactive power compensation. The small value rating of the Active Power Filter (APF) and tuned LC passive filter are combined to form Shunt Hybrid Passive Filter. The Shunt Passive Filter (SPF) consists of tuned LC filter and TCR which is used to counterbalance reactive power in the system. Here APF is utilized to ameliorate the filter capability of SPF and to inhibit the beingness of resonance between the line inductance and the SPF.

The PI controller and the Lookup table are used to educe the firing angle for the TCR according to the reactive power requirement in the system. This firing angle varies the susceptance value of the LC filter. By adjusting the Capacitance value in the passive filter, the reactive power is fed to the system. The SHPF is controlled using Non-Linear Control technique. In this control technique, system current is tracked and the voltage regulation is carried out. It mainly depends upon Decoupling control strategy which makes use of the controlled system into inner current loop control and outer voltage loop control. The SHPF injects currents into the system and it is controlled by the Decoupled Control Strategy with the help of the synchronous orthogonal frame. The SHPF is capable of maintaining the DC bus voltage at a constant value of 50V at the APF side.

The PI and Non-Linear control strategies are made to work more efficaciously for mitigation of harmonics in the source current and for the reactive power compensation at the load using MATLAB simulation. The THD level at the source side is reduced and attained according to the IEEE-519 standard. In this proposed model, APF is made to control in two different control strategies such as Non-Linear Control technique and with Synchronous Reference Frame (SRF) technique. And which of this control strategy is best among the two techniques is compared in this paper.

System conformation of SHPF-TCR Compensator

The fig.1 demonstrates the topology of the suggested combined SHPF and TCR. The SHPF comprises of a small rating APF which is connected in series with fifth harmonic tuned passive LC filter. The APF which is used here comprises of a 3Φ fully controlled voltage sourced Inverter with a boost inductor in series and a DC capacitor (C_{dc}) as a source. The APF is capable of operating in very low fundamental voltages and currents. Because of this purpose, the rated capacity of the APF is reduced greatly in this proposed model and made to work in coordination with the TCR for compensating the reactive power requirement in the system and for the mitigation of harmonics in the source current. The fifth harmonic tuned passive filter is shunted with TCR to form a Shunt Passive Filter (SPF). This passive filter arrangement is mainly for mitigation of harmonics and for the power factor correction in the system. The APF has the capability of eradicating existence of resonance amongst the grid inductance and the SPF. The main aim of the TCR is to compensate the reactive power.

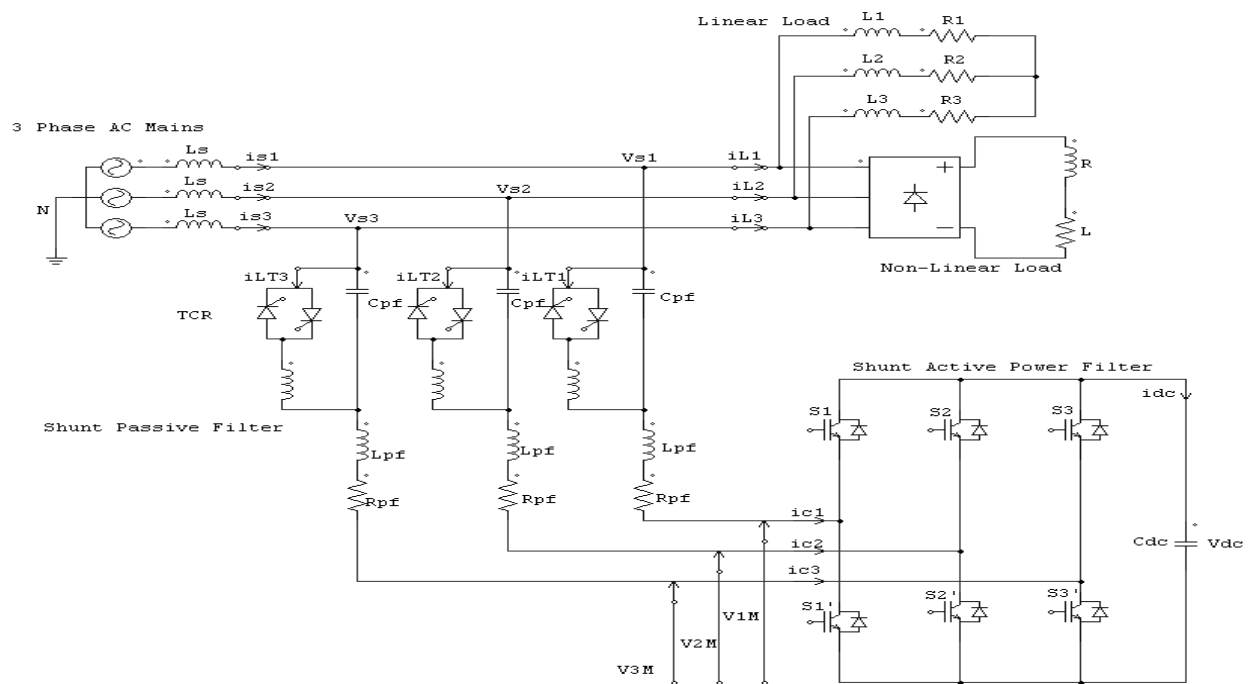


Figure 1: Demonstrates the topology of the suggested combined SHPF and TCR

Modeling of Control Strategy

A. Modeling of The SHPF

The system equations are neatly explained in the 123 reference frame type.

Using Kirchhoff's Voltage law to the figure1, we can write it as follows

$$\begin{aligned} V_{s1} &= L_{pf} \frac{di_{c1}}{dt} + R_{pf} i_{c1} + V_{CPF1} + V_{1M} + V_{MN} \\ V_{s2} &= L_{pf} \frac{di_{c2}}{dt} + R_{pf} i_{c2} + V_{CPF2} + V_{2M} + V_{MN} \\ V_{s3} &= L_{pf} \frac{di_{c3}}{dt} + R_{pf} i_{c3} + V_{CPF3} + V_{3M} + V_{MN} \\ \frac{dV_{dc}}{dt} &= \frac{1}{C_{dc}} i_{dc} \end{aligned} \quad (1)$$

The C_u represents the switching function of the C^{th} leg of the converter for which $u = 1, 2, 3$ is delineated as

$$C_u = \begin{cases} 1, & \text{if } S_u \text{ is On and } S'_u \text{ is off} \\ 0, & \text{if } S_u \text{ is Off and } S'_u \text{ is On.} \end{cases} \quad (2)$$

The d_{nu} represents the state function and it is delineated as

$$d_{nu} = ((C_u) - \frac{1}{3} \sum_{m=1}^3 C_m) \quad (3)$$

Furthermore, the missing of the zero sequence in the AC currents and in the voltages and in the $[d_{nu}]$ functions directs to the corresponding transmuted model in the three phase co-ordinates as shown below.

$$\begin{aligned} L_{pf} \frac{di_{c1}}{dt} &= -R_{pf} i_{c1} - d_{n1} V_{dc} - V_{CPF1} + V_{s1} \\ L_{pf} \frac{di_{c2}}{dt} &= -R_{pf} i_{c2} - d_{n2} V_{dc} - V_{CPF2} + V_{s2} \\ L_{pf} \frac{di_{c3}}{dt} &= -R_{pf} i_{c3} - d_{n3} V_{dc} - V_{CPF3} + V_{s3} \\ C_{dc} \frac{dV_{dc}}{dt} + \frac{V_{dc}}{R_{dc}} &= d_{n1} i_{c1} + d_{n2} i_{c2} + d_{n3} i_{c3} \end{aligned} \quad (4)$$

The above equation (4) is transformed in to the corresponding Synchronous orthogonal frame by make use of the general matrix transformation principle as shown below

$$C_{dq}^{123} = \sqrt{\frac{2}{3}} \begin{bmatrix} \cos \theta & \cos \left(\theta - \frac{2\pi}{3} \right) & \cos \left(\theta - \frac{4\pi}{3} \right) \\ -\sin \theta & -\sin \left(\theta - \frac{2\pi}{3} \right) & -\sin \left(\theta - \frac{4\pi}{3} \right) \end{bmatrix} \quad (5)$$

Where $\theta = \omega t$ and the following equations holds

$$C_{123}^{dq} = (C_{dq}^{123})^{-1} = (C_{dq}^{123})^T$$

After by applying the dq transformation principle, the system state space model used in the synchronous reference frame theory is derived below

$$\begin{aligned}
\frac{di_d}{dt} &= \frac{1}{(L_{pf}(1 - C_{pf}L_T\omega^2) + L_T)} \left[-R_{pf}(1 - C_{pf}L_T\omega^2)i_d \right. \\
&\quad + \omega(L_{pf}(1 - C_{pf}L_T\omega^2) + L_T)i_q - 2\omega C_{pf}L_{pf} \frac{dV_{CPFq}}{dt} \\
&\quad \left. + C_{pf}L_T \frac{d^2V_{CPFd}}{dt^2} - (1 - C_{pf}L_T\omega^2)d_{nd}V_{dc} + (1 - C_{pf}L_T\omega^2)V_d \right] \\
\frac{di_q}{dt} &= \frac{1}{(L_{pf}(1 - C_{pf}L_T\omega^2) + L_T)} \left[-R_{pf}(1 - C_{pf}L_T\omega^2)i_q \right. \\
&\quad + \omega(L_{pf}(1 - C_{pf}L_T\omega^2) + L_T)i_d - 2\omega C_{pf}L_{pf} \frac{dV_{CPFd}}{dt} \\
&\quad \left. + C_{pf}L_T \frac{d^2V_{CPFq}}{dt^2} - (1 - C_{pf}L_T\omega^2)d_{nq}V_{dc} + (1 - C_{pf}L_T\omega^2)V_q \right] \\
\frac{dV_{dc}}{dt} &= \frac{d_{nd}}{C_{dc}}i_d + \frac{d_{nq}}{C_{dc}}i_q - \frac{V_{dc}}{R_{dc}C_{dc}}
\end{aligned} \tag{A}$$

The above equation clearly shows that the model is non-linear in nature because of the beingness of multiplication terms amongst the state variables $\{i_d, i_q, V_{dc}\}$ and the switching state function $\{d_{nd}, d_{nq}\}$. Nevertheless, the model shown is invariant on a switching state of the system.

Moreover, the three state variables have to be controlled independently for the efficacious operation of the SHPF. The interaction amongst the inner current loop control and the outer DC bus voltage loop control can be averted by frequently dissevering their respective dynamics.

B. Current Harmonic Control

Here the fast inner current loop control and slow outer voltage loop control is acquired. The two equations of the systems in the Synchronous Reference Frame can also be written as

$$\begin{aligned}
\frac{di_d}{dt} + \frac{R_{pf}(1 - C_{pf}L_T\omega^2)}{(L_{pf}(1 - C_{pf}L_T\omega^2) + L_T)}i_d \\
&= \frac{1}{(L_{pf}(1 - C_{pf}L_T\omega^2) + L_T)} \left[\omega(L_{pf}(1 - C_{pf}L_T\omega^2) + L_T)i_q \right. \\
&\quad - 2\omega C_{pf}L_T \frac{dV_{CPFq}}{dt} + C_{pf}L_T \frac{d^2V_{CPFd}}{dt^2} - (1 - C_{pf}L_T\omega^2)d_{nd}V_{dc} \\
&\quad \left. + (1 - C_{pf}L_T\omega^2)V_d \right]
\end{aligned}$$

$$\begin{aligned}
\frac{di_q}{dt} + \frac{R_{pf}(1 - C_{pf}L_T\omega^2)}{(L_{pf}(1 - C_{pf}L_T\omega^2) + L_T)}i_q \\
= \frac{1}{(L_{pf}(1 - C_{pf}L_T\omega^2) + L_T)} \left[-\omega(L_{pf}(1 - C_{pf}L_T\omega^2) + L_T)i_d \right. \\
+ 2\omega C_{pf}L_T \frac{dV_{CPFd}}{dt} + C_{PF}L_T \frac{d^2V_{CPFq}}{dt^2} - (1 - C_{pf}L_T\omega^2)d_{nq}V_{dc} \\
\left. + (1 - C_{pf}L_T\omega^2)V_q \right]
\end{aligned} \tag{B}$$

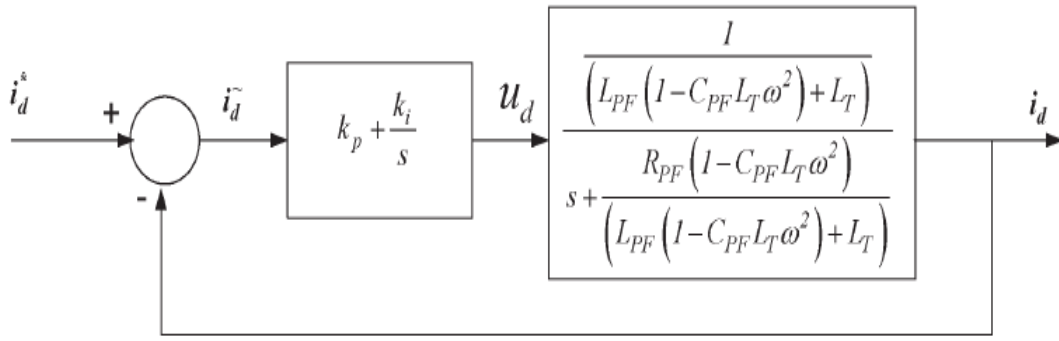


Figure 2: Inner current loop control of i_d

It is mentioned from the first and second time derivatives of the TCR Shunt capacitor Voltages have no substantial negative encroachment on the functioning of the proposed control strategy. This is due to their co-efficient values are comparatively very low and it can be ignored practically. Their equivalent inputs can be written as follows.

$$\begin{aligned}
u_d &= \frac{1}{(L_{pf}(1 - C_{pf}L_T\omega^2) + L_T)} \left[\omega(L_{pf}(1 - C_{pf}L_T\omega^2) + L_T)i_q \right. \\
&\quad \left. - (1 - C_{pf}L_T\omega^2)d_{nd}V_{dc} + (1 - C_{pf}L_T\omega^2)V_d \right] \\
u_q &= \frac{1}{(L_{pf}(1 - C_{pf}L_T\omega^2) + L_T)} \left[\omega(L_{pf}(1 - C_{pf}L_T\omega^2) + L_T)i_d \right. \\
&\quad \left. - (1 - C_{pf}L_T\omega^2)d_{nq}V_{dc} + (1 - C_{pf}L_T\omega^2)V_q \right]
\end{aligned} \tag{C}$$

The decoupled dynamics of the current tracking is achieved with the help of the following transformation of the system model. The dc component i_d and i_q currents can be controlled independently. Moreover, the fast dynamic response of the model and the zero steady state error in the system can be easily obtained with the help of the proportional integral compensators. The controllers can be effectively tracked using the following expressions. Such as

$$\begin{aligned}
 u_d &= (L_{pf}(1 - C_{pf}L_T\omega^2) + L_T)\frac{di_d}{dt} + R_{pf}(1 - C_{pf}L_T\omega^2)i_d \\
 u_d &= K_p\tilde{i}_d + K_i \int \tilde{i}_d dt \\
 u_q &= (L_{pf}(1 - C_{pf}L_T\omega^2) + L_T)\frac{di_q}{dt} + R_{pf}(1 - C_{pf}L_T\omega^2)i_q \\
 u_q &= K_p\tilde{i}_q + K_i \int \tilde{i}_q dt
 \end{aligned} \tag{6}$$

Where $\tilde{i}_d = i_d^* - i_d$ and $\tilde{i}_q = i_q^* - i_q$ are the errors in the current and i_d^* and i_q^* represents the reference current signals of i_d and i_q correspondingly.

The proportional integral transfer function is written as

$$\begin{aligned}
 G_{i1}(s) &= \frac{u_d(s)}{\tilde{i}_d(s)} = K_{p1} + \frac{K_{i1}}{s} \\
 G_{i2}(s) &= \frac{u_q(s)}{\tilde{i}_q(s)} = K_{p2} + \frac{K_{i2}}{s}
 \end{aligned} \tag{7}$$

The inner current loop control i_d is depicted clearly in the figure.2.

The closed loop transfer function of the inner current loops are written as

$$\begin{aligned}
 \frac{I_d(s)}{I_d^*(s)} &= \frac{K_{p1}}{A} \frac{\left(s + \frac{K_{i1}}{K_{p1}}\right)}{s^2 + \left(\frac{B+K_{p1}}{A}\right)s + K_{i1}} \\
 \frac{I_q(s)}{I_q^*(s)} &= \frac{K_{p2}}{A} \frac{\left(s + \frac{K_{i2}}{K_{p2}}\right)}{s^2 + \left(\frac{B+K_{p2}}{A}\right)s + K_{i2}}
 \end{aligned} \tag{8}$$

Where $A = L_{pf}(1 - C_{pf}L_T\omega^2) + L_T$ and $B = R_{pf}(1 - C_{pf}L_T\omega^2)$.

The closed loop transfer function of the inner current loop has the respective forms as

$$\frac{I_d(s)}{I_d^*(s)} = 2\zeta\omega_{ni} \frac{s + \frac{\omega_{ni}}{2\zeta}}{s^2 + 2\zeta\omega_{ni}s + \omega_{ni}^2} \tag{9}$$

Where ω_{ni} is the inner current loop natural angular frequency and ζ is the damping factor. For the given optimal value of the damping factor $\zeta = \frac{\sqrt{2}}{2}$, the theoretical peak overshoot is 20.79%. The K_p and K_i are co-related as follows

$$\begin{aligned}
 K_{p1} &= K_{p2} = 2\zeta\omega_{ni}(L_{pf}(1 - C_{pf}L_T\omega^2) + L_T) - R_{pf}(1 - C_{pf}L_T\omega^2) \\
 K_{i1} &= K_{i2} = (L_{pf}(1 - C_{pf}L_T\omega^2) + L_T)\omega_{ni}^2
 \end{aligned}$$

The control law is given as

$$d_{nd} = \frac{1}{(1 - C_{pf}L_T\omega^2)V_{dc}} [\omega(L_{pf}(1 - C_{pf}L_T\omega^2) + L_T)i_q + (1 - C_{pf}L_T\omega^2)V_d - (L_{pf}(1 - C_{pf}L_T\omega^2) + L_T)u_d] \quad (D)$$

$$d_{nq} = \frac{1}{(1 - C_{pf}L_T\omega^2)V_{dc}} [-\omega(L_{pf}(1 - C_{pf}L_T\omega^2) + L_T)i_d + (1 - C_{pf}L_T\omega^2)V_q - (L_{pf}(1 - C_{pf}L_T\omega^2) + L_T)u_q] \quad (E)$$

The above equations (D) and (E) have the variable d_{nd} and d_{nq} whose input consists of non-linearity cancellation portion and the linear decoupling compensation part.

C. DC Bus Voltage Regulation

For maintaining the DC bus voltage at the APF to a desired value, the i_q component in the controller is varied. This variation in i_q component is done with the help of the Hybrid power filter components in the system.

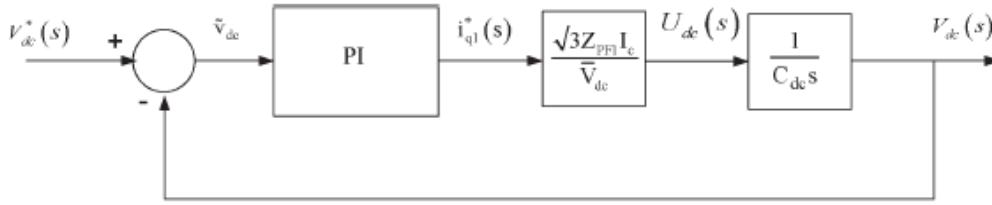


Fig.3.Outer voltage loop control

The sensed DC bus voltage and the desired reference voltage is compared and added with the q component of the reference current i_q as depicted in the figure. The final equation of the model depicted in the equation 4 is modified and written as

$$C_{dc} \frac{dv_{dc}}{dt} + \frac{V_{dc}}{R_{dc}} = d_{nq}i_q \quad (10)$$

The three-phase filter currents are written as

$$\begin{bmatrix} i_{c1} \\ i_{c2} \\ i_{c3} \end{bmatrix} = \sqrt{\frac{2}{3}} i_q \begin{bmatrix} -\sin \theta \\ -\sin \left(\theta - \frac{2\pi}{3} \right) \\ -\sin \left(\theta - \frac{4\pi}{3} \right) \end{bmatrix} \quad (11)$$

The fundamental filter RMS current I_c is

$$I_c = \frac{i_q}{\sqrt{3}} \quad (12)$$

The q- axis Active power filter Voltage is uttered as

$$V_{Mq} = q_{nq}V_{dc} = -Z_{pf1}i_{q1}^* \quad (13)$$

Where Z_{pf1} is termed as the impedance of the shunt passive filter at 50Hz and i_{q1}^* is a dc component in the system.

The relative input u_{dc} is termed as

$$u_{dc} = q_{nq} i_q \quad (14)$$

The reference current of the DC bus voltage loop is termed as

$$i_q^* = \frac{V_{dc}}{-Z_{pf1} i_q} u_{dc} \quad (15)$$

The dc component of the reference current will coerce the SHPF-TCR compensator to generate or to extract current at the fundamental frequency.

In order to regularize the dc bus voltage V_{dc} , the error difference signal $\tilde{V}_{dc} = V_{dc}^* - V_{dc}$ is made to pass through a Proportional Integral controller is clearly shown in the figure 3.

$$u_{dc} = K_1 \tilde{V}_{dc} + K_2 \int \tilde{V}_{dc} dt \quad (16)$$

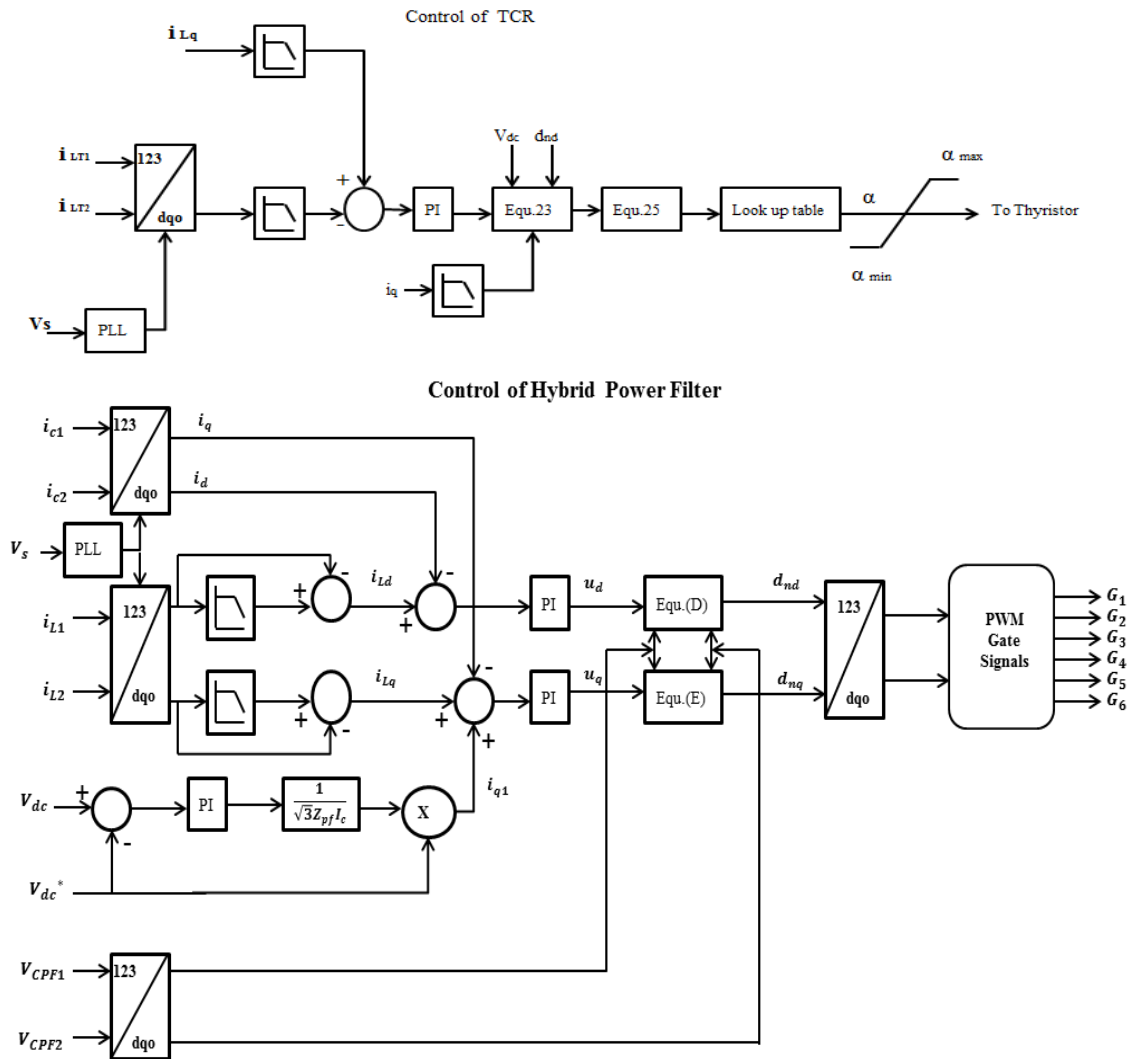


Figure 4: Control strategy of the SHPF-TCR compensator

SRF Control Strategy

The term SRF means Synchronous Reference Frame. The control strategy is modeled using Synchronous Reference Frame theory. Hence this control strategy is named as SRF controller. This controller is mainly used for controlling the harmonic current compensation purpose which is used in the real-time execution in Active Power Filter (APF) circuit. The SHPF-TCR is also tested with the SRF controller and its performance is acutely analyzed. The PWM pulses are generated with the help of the SRF Controller and it is fed to the VSI in the APF module. The main purpose of the SRF controller is to control the current harmonics in the system. The DC bus voltage should be retained constant with help of the PI- controller for furnishing the DC power to the VSI in the APF.

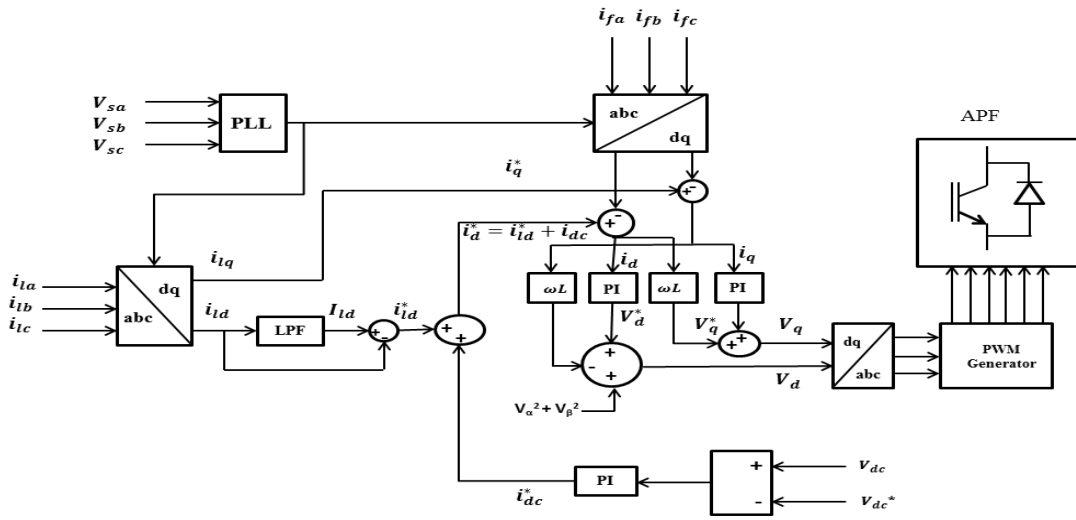


Figure 7: Represents the Control of APF using SRF Control Strategy

The instantaneous supply voltage is

$$V_{s1} = V_m \sin(\omega t)$$

$$V_{s2} = V_m \sin(\omega t - 120^\circ)$$

$$V_{s3} = V_m \sin(\omega t - 240^\circ)$$

The instantaneous three phase voltage can be transformed into two phase stationary components dq voltages with the help of the Clarke's Transformation as follows

$$\begin{bmatrix} V_d \\ V_q \end{bmatrix} = \sqrt{\frac{2}{3}} \begin{bmatrix} 1 & -1/2 & -1/2 \\ 0 & \sqrt{3}/2 & -\sqrt{3}/2 \end{bmatrix} \begin{bmatrix} V_{s1} \\ V_{s2} \\ V_{s3} \end{bmatrix} \quad (17)$$

These transformed dq voltage components are allowed to pass through Low-pass Filter hence it eliminates the high frequency noises and it is given as input to the Phase Lock Loop (PLL) block.

The instantaneous load current can also be transformed into two phase stationary components dq currents with the help of the Clarke's Transformation as follows

$$\begin{bmatrix} i_{Ld} \\ i_{Lq} \end{bmatrix} = \sqrt{\frac{2}{3}} \begin{bmatrix} 1 & -1/2 & -1/2 \\ 0 & \sqrt{3}/2 & -\sqrt{3}/2 \end{bmatrix} \begin{bmatrix} i_{s1} \\ i_{s2} \\ i_{s3} \end{bmatrix} \quad (18)$$

The stationary two phase component is transformed into rotating dq reference components as

$$\begin{bmatrix} i_{L1d} \\ i_{L1q} \end{bmatrix} = \begin{bmatrix} \cos \theta & \sin \theta \\ -\sin \theta & \cos \theta \end{bmatrix} \begin{bmatrix} i_{Ld} \\ i_{Lq} \end{bmatrix} \quad (19)$$

These transformed dq current components are allowed to pass through Low-pass Filter hence it eliminates the high frequency noises. The filter current is also transformed in to dq components as i_{f1d} and i_{f1q} .

And these two dq component currents are compared with the error current components formed by the comparison of V_{dc} and V_{dc}^* and finally the error signals are allowed to pass through PI- controllers and V_d and V_q components are obtained.

These dq voltage components are once again transformed into three phase components as 123 components as reference signals ($V_{s1}^*, V_{s2}^*, V_{s3}^*$).

These reference 123 components are compared with actual instantaneous 123 components using operational conditions and generate the pulses for the VSI in the APF for eliminating the current harmonics.

Modeling of TCR

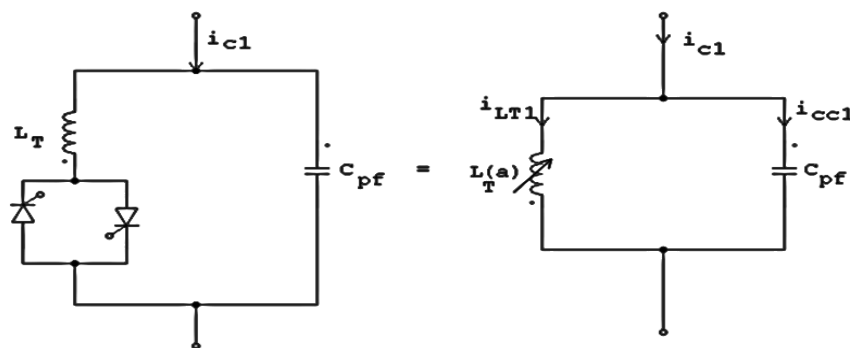


Figure 5: TCR Equivalent Model

The variable inductance is change according to the requirement with the help of the Thyristor triggering angle α . The Kirchhoff's Voltage law is applied to TCR connected Passive filter circuit in 123 reference frame as

$$\begin{aligned}
V_{s1} &= L_T \frac{di_{LT1}}{dt} + L_{pf} \frac{di_{c1}}{dt} + R_{pf} i_{c1} + d_{n1} V_{dc} \\
V_{s2} &= L_T \frac{di_{LT2}}{dt} + L_{pf} \frac{di_{c2}}{dt} + R_{pf} i_{c2} + d_{n2} V_{dc} \\
V_{s3} &= L_T \frac{di_{LT3}}{dt} + L_{pf} \frac{di_{c3}}{dt} + R_{pf} i_{c3} + d_{n3} V_{dc}
\end{aligned} \tag{20}$$

After applying the Park's Transformation in the above equation 20, we get as

$$\begin{aligned}
L_T(\alpha) \frac{di_{LTd}}{dt} &= L_T(\alpha) \omega i_{LTq} + L_{pf} \omega i_q - L_{pf} \frac{di_d}{dt} - R_{pf} i_d - d_{nd} V_{dc} + V_d \\
L_T(\alpha) \frac{di_{LTq}}{dt} &= L_T(\alpha) \omega i_{LTd} + L_{pf} \omega i_d - L_{pf} \frac{di_q}{dt} - R_{pf} i_q - d_{nq} V_{dc} + V_q
\end{aligned} \tag{21}$$

Only the reactive part in the equation is preferred to control reactive current, hence $V_q = 0$ and $L_T(\alpha) \frac{di_{LTd}}{dt} = 0$ is applied. Now the above equation 20 becomes

$$\frac{di_{LTq}}{dt} = B(\alpha) \omega \left[-L_{pf} \omega i_d - L_{pf} \frac{di_q}{dt} - R_{pf} i_q - d_{nq} V_{dc} \right] \tag{22}$$

Where $B(\alpha) = \frac{1}{L_{pf} \omega}$ is the susceptance value.

The input $u_q T$ is termed as

$$u_q T = \frac{di_{LTq}}{dt} \tag{23}$$

Based on the above derived expression, we deduce

$$B(\alpha) = \frac{u_q T}{\omega \left[-L_{pf} \omega i_d - L_{pf} \frac{di_q}{dt} - R_{pf} i_q - d_{nq} V_{dc} \right]} \tag{24}$$

Similarly, the equivalent inductance in the TCR compensator circuit is expressed as

$$L_{pf}(\alpha) = L_{pf} \frac{\pi}{(2\pi - 2\alpha + \sin(2\alpha))} \tag{25}$$

The susceptance value calculated using the following expression

$$B(\alpha) = B \frac{2\pi - 2\alpha + \sin(2\alpha)}{\pi} \tag{26}$$

Where the term $B = \frac{1}{L_{pf} \omega_o}$

The Value of the B is purely dependent on the value of the Inductor used in the Passive Filter.

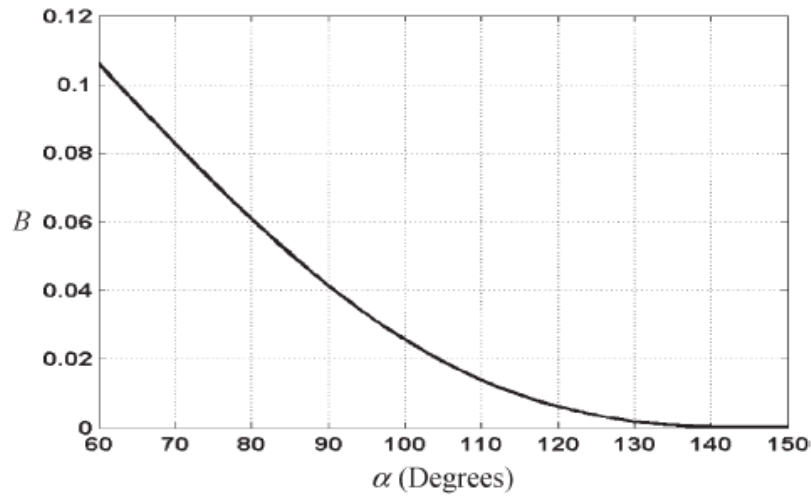


Figure 6: Exemplify the Susceptance (B) versus Firing Angle (α)

Simulation Results

The simulation is carried out using the parameters depicted in Table1 in the MATLAB Simulink software.

Specification of Parameters Table I

| | |
|---|---|
| Line to Line source voltage and frequency | $V_{sLL} = 415V$, $F_s = 50Hz$ |
| Line impedance | $L_s = 0.5mH$, $R_s = 0.1\Omega$ |
| Non linear load | $L_{L1} = 10mH$, $R_{L1} = 27\Omega$ |
| Linear load | $L_{L2} = 20mH$, $R_{L2} = 27\Omega$ |
| Passive filter parameters | $L_{pf} = 1.2mH$, $C_{pf} = 240\mu F$ |
| Active filter parameters | $C_{dc} = 3000\mu F$, $R_{dc} = 1K\Omega$ |
| DC bus voltage of APF of SHAF | $V_{dc} = 50V$ |
| Switching frequency | 1920 Hz |
| Inner controller parameters | $K_{P1} = K_{P2} = 43.38$, $K_{i1} = K_{i2} = 37408$ |
| Outer controller parameters | $K_1 = 0.26$, $K_2 = 42$ |
| Cut off frequency of the low pass filters | $F_c = 70Hz$ |
| TCR inductance | $L_T = 25mH$ |

The SHPF compensating proposed model is simulated in MATLAB simulink using two control strategies such as Non-Linear Control strategy and SRF control strategy. The TCR is simulated using PI- Control strategy with both the above mentioned control strategies. The SHPF performance is analyzed deeply with two control strategies and the THD levels at the source current are reduced largely.

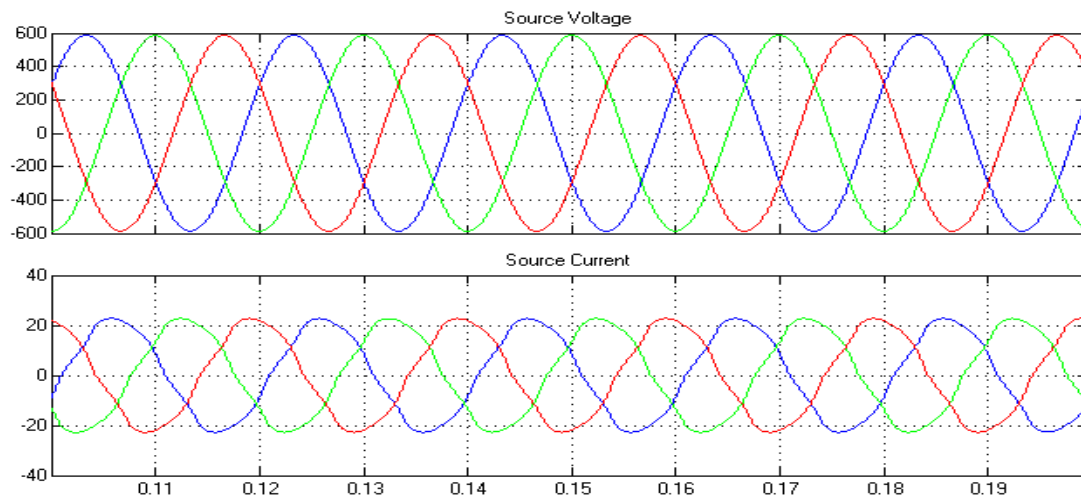


Figure 7: Waveform of Source Voltage and Source Current with Non-linear Controller and PI-Controller

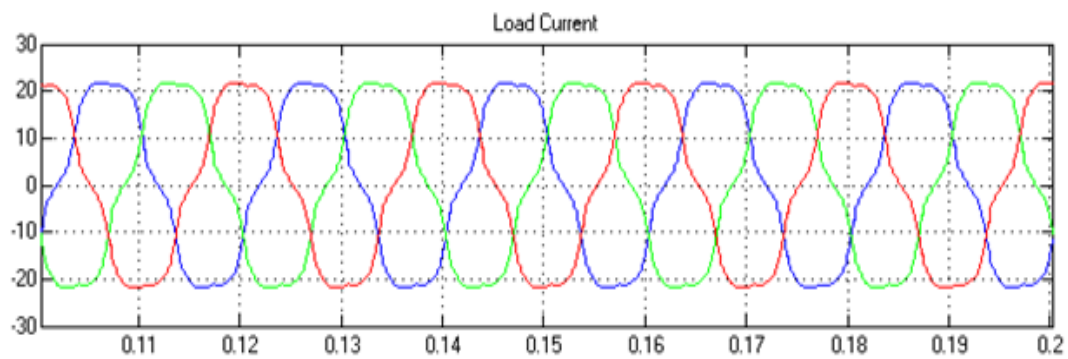


Figure 8: Waveform of Load Current with Non-linear Controller and PI-Controller

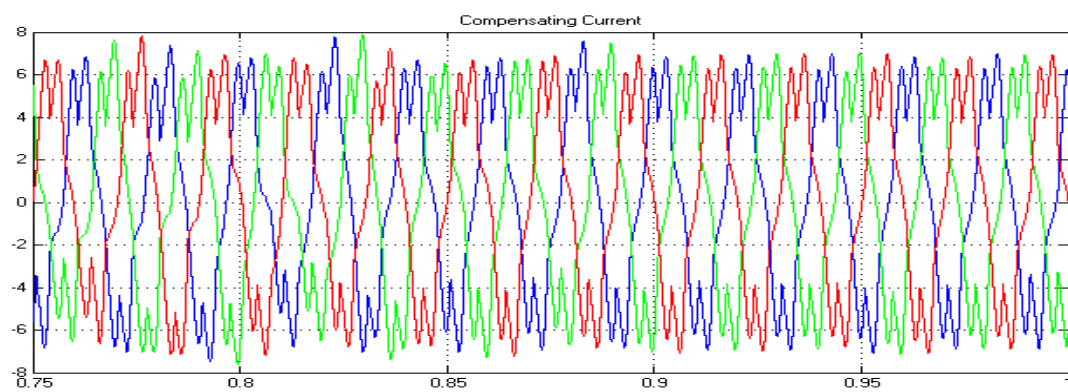


Figure 9: Waveform of Compensating Current with Non-linear Controller and PI-Controller

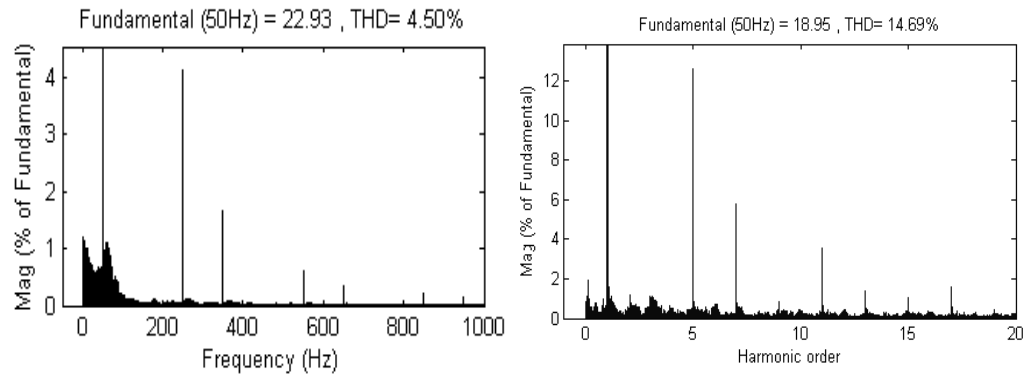


Figure 10: THD Levels of the Source and Load Current with Non-linear Controller and PI-Controller

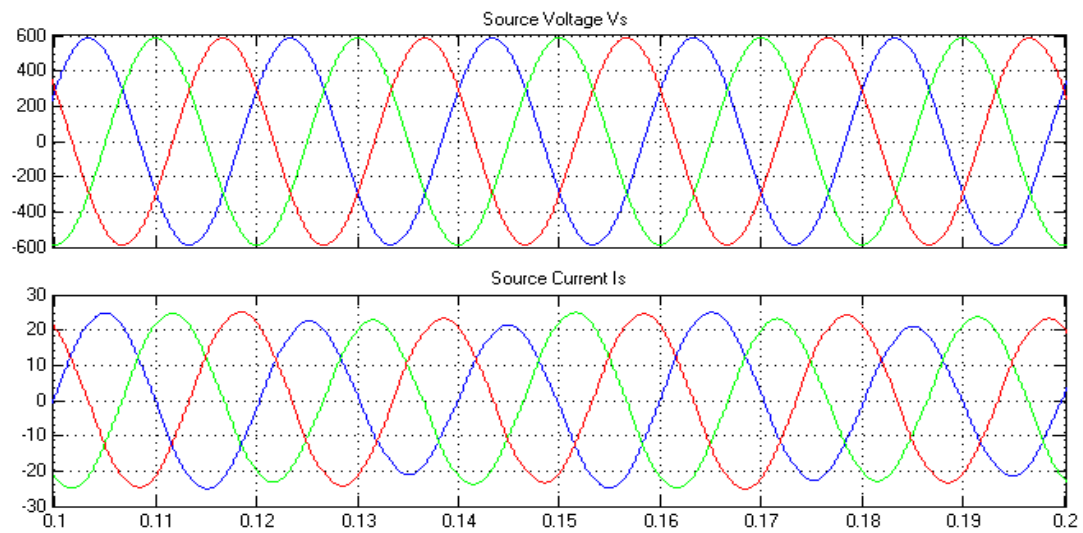


Figure 11: Waveform of Source Voltage and Source Current with SRF Controller and PI-Controller

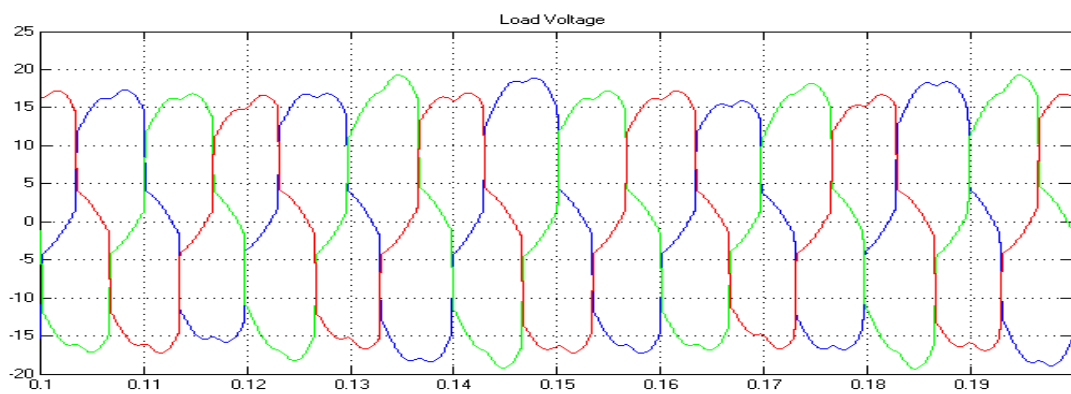


Figure 12: Waveform of Load Current with SRF Controller and PI-Controller

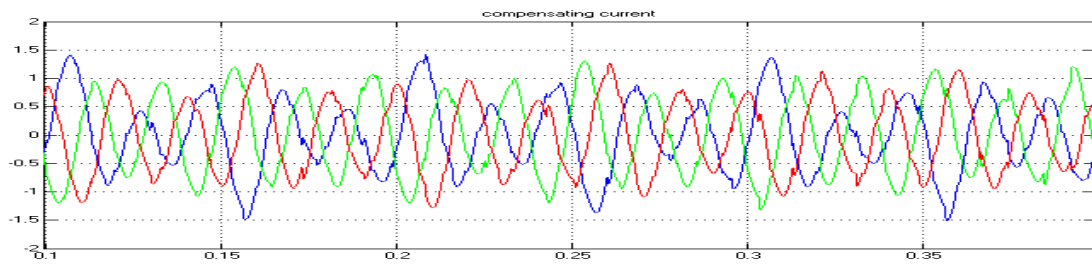


Figure 13: Waveform of Compensating Current with SRF Controller and PI-Controller

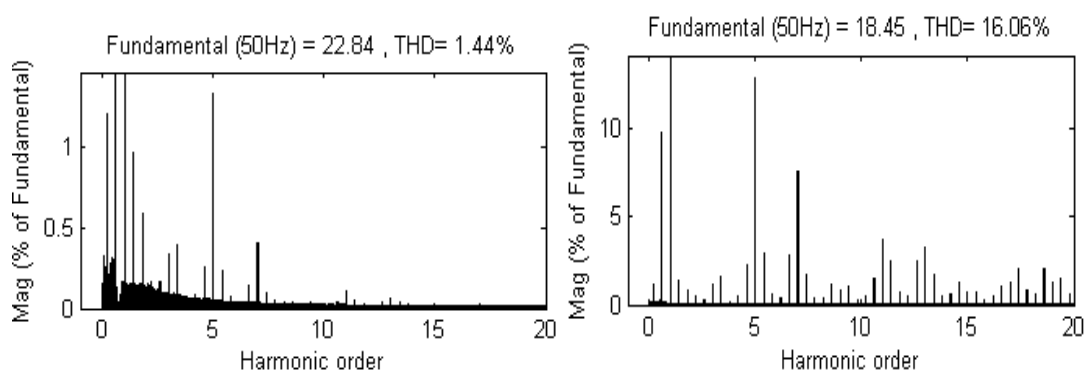


Figure 14: THD Levels of the Source and Load Current with Non-linear Controller and PI-Controller

| Case | Description | Source THD (%) | Load THD (%) |
|------|--|----------------|--------------|
| 1 | System with Non-Linear Load with SHPF-TCR Compensation using Non-Linear Controller and PI-Controller | 4.5 | 14.69 |
| 2 | System with Non-Linear Load with SHPF-TCR Compensation using SRF Controller and PI-Controller | 1.44 | 16.06 |

Performance analysis Table II

From the table II, it is inferred that reactive power compensation for the system with Non-Linear load is analyzed using Decoupled Feedback Linearization Controller and SRF controller techniques. Using DFL technique, the %THD is reduced from 14.69% to 4.5% whereas in SRF technique, the %THD is reduced from 16.06% to 1.44%. The SRF control technique performs better in mitigating the harmonics in the source current than DFL control technique. The steady state response of the SRF control technique is quite faster for maintaining the quality of the system.

Conclusion

With this paper, the designed SHPF-TCR compensator and its performance are explicated neatly. The SHPF response for mitigation of harmonics and reactive power compensation has been enhanced by implementing two different control strategies. Here the SHPF is composed of an Active Power Filter (APF) in series with a Passive Filter has a dual task of ameliorating the performance of filtering capability and decreases the power rating of the Active Filter in the system and there by reduces the cost. The performances of the SHPF with two control strategies are analyzed separately, by making it to work with TCR PI-control strategy and with same source and load conditions. With the help of these control strategies, the %THD level at source current is reduce to the IEEE-519 standard which is to be less than 5%. The same %THD is achieved with the help of the SHPF-TCR compensator. Both the control strategies have mitigated the current harmonics according to IEEE standard. The SRF control strategy has better performance as compared with the Non-Linear Control strategy in both steady as well as dynamic states. The compensator has good dynamic response in compensating the reactive power requirement and in eliminating the harmonics in the source current.

References

- [1] Hamadi, S. Rahmani, and K. Al-Haddad, Jul. 2010, "A hybrid passive filter configuration for VAR control and harmonic compensation," *IEEE Trans. Ind. Electron.*, 57 (7), pp. 2419–2434.
- [2] Salem Rahmani, Kamal Al-Haddad and Louis A. Dessaint, "A Combination of Shunt Hybrid Power Filter and Thyristor-Controlled Reactor for Power Quality, Jan. 2009," *IEEE Trans. Ind. Electron.*, 61(5), pp. 2152–2164.
- [3] H. Hu, W. Shi, Y. Lu, and Y. Xing, Sep. 2012, "Design considerations for DSP controlled 400 Hz shunt active power filter in an aircraft power system," *IEEE Trans. Ind. Electron.*, 59(9), pp. 3624–3634.
- [4] X. Du, L. Zhou, H. Lu, and H.-M. Tai, Mar. 2012, "DC link active power filter for three-phase diode rectifier," *IEEE Trans. Ind. Electron.*, 59(3), pp. 1430–1442.
- [5] M. Angulo, D. A. Ruiz-Caballero, J. Lago, M. L. Heldwein, and S. A. Mussa, Jul. 2013, "Active power filter control strategy with implicit closed-loop current control and resonant controller," *IEEE Trans. Ind. Electron.*, 53 (7), pp. 2721–2730.
- [6] J. A. Munoz, J. R. Espinoza, C. R. Baier, L. A. Moran, E. E. Espinosa, P. E. Melin, and D. G. Sbarbaro, Oct. 2012 "Design of a discrete-time linear control strategy for a multicell UPQC," *IEEE Trans. Ind. Electron.*, vol. 59(10), pp. 3797–3807.
- [7] Y. Tang, P. C. Loh, P. Wang, F. H. Choo, F. Gao, and F. Blaabjerg, Mar. 2012 "Generalized design of high performance shunt active power filter

- with output LCL filter,” *IEEE Trans. Ind. Electron.*, vol. 59(3), pp. 1443–1452.
- [8] S. Lam, W. H. Choi, M. C. Wong, and Y. D. Han, “Adaptive dc-link voltage-controlled hybrid active power filters for reactive power compensation,” *IEEE Trans. Power Electron.*, vol. 27(4), pp. 1758–1772.